# *Comptes Rendus*

# *Mécanique*

Gergely Molnár, Aurélien Doitrand, Rafael Estevez and Anthony Gravouil

**A review of characteristic lengths in the coupled criterion framework and advanced fracture models**

Review article / *Article de synthèse*

# A review of characteristic lengths in the coupled criterion framework and advanced fracture models

## *Une revue des longueurs caractéristiques dans le cadre du critère couplé et dans les modèles de fracture avancés*

**Gergely Molnár** [®],[*],[a]**, Aurélien Doitrand** [®],[*],[b]**, Rafael Estevez** [®],[c] **and Anthony Gravouil** [®],[d]

[a] CNRS, INSA Lyon, LaMCoS, UMR5259, 69621 Villeurbanne, France

[b] Université Lyon, INSA-Lyon, UCBL, CNRS, MATEIS, UMR5510, F-69621 Villeurbanne, France

[c] Univ. Grenoble Alpes, CNRS, Grenoble INP, SIMAP, F-38000 Grenoble, France

[d] Univ Lyon, CNRS, INSA Lyon, LaMCoS, UMR5259, 69621 Villeurbanne, France

*E-mails:* gergely.molnar@insa-lyon.fr (G. Molnár), aurelien.doitrand@insa-lyon.fr (A. Doitrand), rafael.estevez@grenoble-inp.fr (R. Estevez), anthony.gravouil@insa-lyon.fr (A. Gravouil)

**Abstract.** The review paper explores the significance of characteristic lengths in fracture mechanics, focusing on the Coupled Criterion framework. It addresses limitations in traditional Linear Elastic Fracture Mechanics, which struggle to predict small-scale crack behaviors, and highlights the need for models that allow characteristic lengths to emerge from material properties and geometry rather than being predefined inputs.

The review covers two main characteristic lengths: the initiation crack length and Irwin's length, examining their interactions with lengths used in other fracture approaches such as Phase-Field methods, Cohesive Zone Models, and atomic-scale simulations. The findings show that Irwin's length consistently appears in models that combine stress and energy criteria, indicating its fundamental role in fracture prediction.

The study identifies limitations in current models, especially in cases involving strong singularities or where the energy condition dominates, and suggests improvements by incorporating process zone descriptions or regularization techniques from Phase-Field models. These enhancements could better capture the complex behaviors at smaller scales.

The paper concludes by advocating for a combined approach that integrates various fracture models, which could provide a more comprehensive understanding of crack initiation and propagation across different scales. This integrative strategy would allow for more accurate predictions and a deeper insight into the mechanics of fracture.

**Résumé.** Cet article de revue explore l'importance des longueurs caractéristiques en mécanique de la rupture, en se concentrant sur le cadre du Critère Couplé. Il met en lumière les limites des approches traditionnelles de la mécanique de la rupture élastique linéaire, qui peinent à prédire les comportements des fissures à petite échelle, et souligne le besoin de modèles permettant aux longueurs caractéristiques d'émerger des propriétés des matériaux et de la géométrie, plutôt que d'être définies a priori.

*Corresponding authors

La revue couvre deux longueurs caractéristiques principales : la longueur de fissure d'initiation et la longueur d'Irwin, en examinant leurs interactions avec les longueurs utilisées dans d'autres approches de rupture, telles que les méthodes de champ de phase, les modèles de zone cohésive et les simulations à l'échelle atomique. Les résultats montrent que la longueur d'Irwin apparaît systématiquement dans les modèles combinant des critères de contrainte et énergétique, soulignant son rôle fondamental dans la prédiction de la rupture.

L'étude identifie les limites des modèles actuels, en particulier dans les cas impliquant des singularités fortes ou lorsque la condition énergétique domine, et propose des améliorations en incorporant des descriptions de zone de processus ou des techniques de régularisation issues des modèles de champ de phase. Ces améliorations pourraient mieux capturer les comportements complexes à des plus petites échelles.

L'article conclut en prônant une approche combinée intégrant divers modèles de rupture, ce qui pourrait offrir une compréhension plus complète de l'initiation et de la propagation des fissures à différentes échelles. Cette stratégie intégrative permettrait des prédictions plus précises et une compréhension approfondie des mécanismes de la rupture.

## 1. Introduction

Linear Elastic Fracture Mechanics (LEFM), introduced by Griffith [1, 2], addresses the limitations of traditional mechanics in predicting failure in structures containing sharp defects. Stress-based methods suffice for smooth, flaw-free materials, but they fail around cracks, where stresses theoretically peak to infinity. Griffith's energy-based approach relies on the energy release rate to predict crack growth, thus avoiding the consideration of stress singularities. However, LEFM assumes a defect large enough to disregard smaller-scale phenomena near the crack tip, leading to the concept of a non-linear transition length scale, which defines the boundary between the linear elastic region and more complex fracture processes like plasticity or other dissipative mechanisms.

Despite its effectiveness for large cracks, LEFM cannot fully capture behaviors at this smaller scale. Additionally, most structures are not designed with pre-existing macroscopic cracks, making Griffith's theory impractical in such cases, where it would predict an unrealistic infinite load-bearing capacity. As a result, engineering standards continue to predominantly rely on stress-based criteria for materials where significant defects are not anticipated.

The first empirical observations of the size effect date back to Leonardo da Vinci [3, 4], who noticed that shorter cable segments were stronger than longer ones, though he did not provide a practical explanation for this phenomenon. It was Galileo Galilei who later formulated the correct scaling laws for materials under tension and bending [5], emphasizing how size effects limit the structural integrity of large natural and man-made structures. Centuries later, as iron and steel became more widely used, concerns about brittle fracture grew, prompting early material failure testing [6]. Around the same time, Mariotte [7], through extensive experimentation, suggested that the size effect observed by da Vinci was likely due to internal faults, concluding that larger structural elements have a higher probability of containing weak spots, thus reducing their overall strength.

Alongside the development of fracture mechanics, researchers began exploring statistical theories to explain the power-law scaling observed in experimental data. Peirce [8] introduced the weakest-link model for chains, building on extreme value statistics by Tippett [9]. This line of work reached a milestone with Weibull [10, 11], who developed the Weibull distribution to

model failure probability based on low-strength extremes, establishing a power-law relationship between material strength and failure probability, especially in materials with microscopic flaws or microcracks [12]. This statistical approach has since been applied across various materials and fracture phenomena [13–16]. While widely accepted, in this paper, we focus on a physically-based deterministic approach, recognizing that a combined statistical-deterministic framework can provide a more comprehensive view of material failure across scales.

The non-linear scaling law, first documented by Irwin in the 1950s [17], was initially overlooked or considered a statistical anomaly. Motivated by the observation that large concrete structures (such as dams and bridges) behave differently from small laboratory specimens, Bažant conducted a series of experiments [18]. He eventually published his theoretical explanation in 1986, describing a non-linear scaling law in fracture mechanics [19]. Bažant emphasized the need for non-linear analysis to account for the significant size effects observed in various engineering structures. This phenomenon has since become critical for the design of large-scale composite structures such as ship hulls or structural fuselages, as well as in fields like geotechnical and arctic engineering. For example, evaluating fault slip stability in the Earth's crust involves scale transitions that span multiple orders of magnitude.

Bažant [20] further showed that fracture resistance in many materials deviates from the power-law predictions of linear elastic fracture mechanics, especially when the initial flaw size is smaller than a critical value. In such cases, stress-based criteria should be applied. The existence of this critical length scale has since been demonstrated in various materials, including ceramics [21–24], polymers [25, 26], silica glass [27], silicon carbide [28], fiber composite laminates [29], wood [30], concrete, rock [31], spider silk [32] and even sea ice [33]. However, experimentally demonstrate this non-linear scale transition is challenging, as it requires testing specimens across multiple size ranges.

The transition length scale is often compared to the size of the fracture process zone (FPZ), a region around a crack tip where complex, nonlinear deformation occurs. The FPZ, characterized by a transition from elastic to inelastic behavior, plays a critical role in fracture mechanics. In the 1950s, Irwin [34] and Orowan [35] used X-ray measurements to demonstrate that even in brittle materials, there is evidence of regularization along crack surfaces. They independently concluded that the true critical energy release rate should be several orders of magnitude larger than Griffith's original proposal. Later, Barenblatt [36] and Dugdale [37] theorized that material near the crack yields, and this local cohesive traction limits the otherwise infinite stress peak.

Since then, numerous experimental techniques [38–47] have been developed to measure the size and shape [48] of the FPZ in brittle materials. These studies commonly assume that the FPZ is a damaged region around the crack tip linked to irreversible microstructural changes. The FPZ has been observed in materials such as concrete [49], granite [38], natural faults [50], wood [51], model materials [52], and silica glass [53]. A comprehensive review of the FPZ can be found in the thesis of Brooks [54]. Today, digital image correlation [55] is the primary technique used to quantify the FPZ, although other methods exist for transparent materials like polycarbonate [56] or for X-ray measurement in concrete [45]. Döll and Könczöl [57, 58] used optical interferometry to measure crack tip opening displacement in polymethyl methacrylate, polystyrene, and polycarbonate. Their findings indicate that, for these materials, the experimentally measured opening profile aligns well with predictions from an appropriate Dugdale model.

While the non-linear scaling law is widely accepted, its underlying cause remains a topic of active debate. This is particularly important given the rise of advanced manufacturing techniques that allow the creation of architected materials with structural elements smaller than the critical length scale of bulk materials, resulting in exceptionally strong overall responses [59].

In this review paper, we will explore recent methods and theories that effectively account for this non-linear length scale. This length scale can either be explicitly incorporated as a material parameter or arise through the coupling of different criteria.

Even if well-described by various fracture mechanics models through numerical experiments, it is not always straightforward to explain this transition between strength-based and energy-based descriptions of fracture. This transition is clearly understood using the Coupled Criterion (CC) concept [60], that was proposed to rationalize transverse cracking experiments in laminated composites by Parvizi, Garrett, and Bailey [61]. Their results showed two distinct regimes: for sufficiently thick plies, the strain at crack initiation remained constant, whereas it increased with decreasing ply thickness for thin plies. A criterion based solely on critical stress or strain—first introduced by Lamé and Clapeyron [62]—could only account for the failure of thick plies. Extending this approach to a non-local stress evaluation, either averaged over a finite volume [63] or at a specific distance [64–66]—known as the Theory of Critical Distances [67]—did not explain the increase in strain at failure for thin plies. Since Griffith's energy approach cannot predict crack initiation, an energy-based criterion applied to a finite crack surface increment was introduced, representing crack initiation across the full ply thickness. This idea was already suggested in Aveston and Kelly's model [68] and was later formalized as Finite Fracture Mechanics (FFM) by Hashin [69] and then by Nairn [70], successfully explaining the size effect in thin ply fracture. However, it underestimated the load level for crack initiation in thick plies. Dominique Leguillon [60] eventually proposed combining a non-local stress criterion with an energy criterion applied to a finite crack surface increment, asserting that both conditions must be met simultaneously for crack initiation. This approach effectively explains the transition from tensile strength-driven failure in thick plies to energy release rate-driven failure in thin plies.

The CC highlights that the nonlinear fracture resistance scaling is driven by the ratio between the initial flaw size and the Irwin's length. It results from the initiation length emerging from the coupling between the strength-based and energy-based criteria. Our primary focus will thus be on the CC [60], one of the earliest approaches to offer a mechanics-based explanation for the emergence of a process zone. We will then relate macroscopic theories, such as the theory of critical distances, the Phase-Field method, and the Cohesive Zone Model, to the fundamental concept of the Coupled Criterion. We also demonstrate how approaches that model atomic-scale behavior can bridge the gap between the continuum scale and the actual material properties.

The paper is structured as follows. First, in Section 2 the basics of the Coupled Criterion is presented with particular attention to the emerging length scale. Then in Section 3, we summarize the literature comparing the results of the Coupled Criterion with other theories and numerical methods with allow us to have a length scale explicitly or by emergence. In Section 4, we compare and contrast the results obtained with the methods, highlighting their similarities and differences. Finally, in Section 5, we draw conclusions based on our findings.

## 2. The characteristic lengths in the Coupled Criterion

The Coupled Criterion (CC) [60] is an approach in fracture mechanics that enables us to study fracture analysis in a wide range of applications [71, 72]. The underlying concept of the CC is that crack initiation occurs when two conditions are simultaneously met. The first condition arises from an energy equilibrium between the states before and after crack initiation over a specified surface $S$. This allows for the definition of the incremental energy release rate (IERR), given linear elastic material behavior and negligible inertial effects, as $\mathcal{G}_{\text{inc}} = (\delta W_{\text{ext}} - \delta W_{\text{el}})/S$, where $W_{\text{ext}}$ represents the work done by external forces, $W_{\text{el}}$ the elastic strain energy, and $S$ the crack surface area. The IERR approaches the energy release rate (ERR) $\mathcal{G}$ as the crack surface area approaches zero. The CC model is thus consistent with Linear Elastic Fracture Mechanics
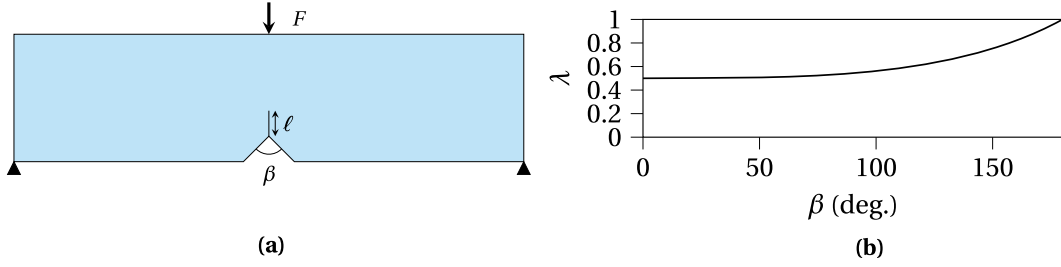
**Figure 1.** (a) Three-point bending of a specimen with a V-notch. (b) Characteristic exponent of the singularity $\lambda$ corresponding to the opening mode as a function of $\beta$, the angle of the V-notch.

(LEFM) for sufficiently long cracks (under LEFM assumptions), while also enabling the study of crack initiation, which LEFM cannot handle as $\mathcal{G}$ tends toward zero when the crack surface tends toward zero. The energy condition for the CC is expressed as:

$$\mathcal{G}_{\text{inc}} \geqslant \mathcal{G}_{\text{c}}, \tag{1}$$

where $\mathcal{G}_{\text{c}}$ is the material's critical ERR.

The second condition of the CC states that the stress along the prospective crack path must be sufficiently large. This introduces a non-local stress criterion, which can be expressed as a function of the stress tensor components and the material strength surface. For a material adhering to a Rankine's strength surface [73], it is given by:

$$\sigma_{\text{nn}}(\mathbf{x}) \geqslant \sigma_{\text{c}} \forall \mathbf{x} \quad \text{in } \Gamma, \tag{2}$$

where $\sigma_{\text{nn}}$ is the stress normal to the crack path $\Gamma$ before initiation, and $\sigma_{\text{c}}$ is the material's tensile strength.

Applying the CC involves combining both the stress and energy conditions to determine the minimum load magnitude at which both criteria are simultaneously met for at least one given crack surface.

An emblematic illustration of the CC is the initiation of a crack at the tip of a V-notch, where the free surfaces form an angle $\beta$, as seen in a notched specimen under bending, illustrated in Figure 1.

The case $\beta = 0°$ corresponds to an initial crack and reverts to LEFM (i.e., crack propagation based solely on energy) provided the crack is sufficiently long [74]. The case $\beta = 180°$ corresponds to a straight edge with no notch; here, the stress is homogeneous, allowing a criterion based on material tensile strength if the specimen is large enough [60, 75]. An asymptotic approach yields the stress normal to the crack path before initiation $\sigma_{\text{nn}}$ and the IERR for a crack of length $\ell$ at the notch tip [76]:

$$\begin{cases} \sigma_{\text{nn}}(r, \theta = 0) = K\ell^{\lambda-1}, \\ \mathcal{G}_{\text{inc}}(\ell) = \dfrac{K^2}{E} \ell^{2\lambda-1} A_{\beta}, \end{cases} \tag{3}$$

where $r$ and $\theta$ are the polar coordinates, $E$ is Young's modulus, and $\lambda$ is an exponent characterizing the singularity, varying between 0.5 for a crack ($\beta = 0°$) and 1 for a straight edge ($\beta = 180°$). In-between cases are presented in Figure 1b. The dimensionless function $A_{\beta}$ depends on the problem's geometry (notably the notch angle $\beta$) and the local loading at the singular point, represented by the generalized stress intensity factor (GSIF) $K$. The GSIF drives the magnitude of the local stress field variation near the V-notch tip. It is a characteristic parameter that can be used to study the nucleation of a crack, i.e., crack initiation occurs when a critical GSIF is reached. It is

calculated based on a path-independent contour integral [76, 77]. Under a linear elastic framework and assuming small deformations, the GSIF is proportional to the applied load $F$, shown in Figure 1a.

If $0 < \beta < 180°$, the stress tends to infinity as $r$ approaches 0, making a stress-based criterion alone ineffective, as it predicts crack initiation under an infinitesimal load. Conversely, the IERR approaches 0 as the crack length approaches 0, meaning an energy-based criterion alone does not predict crack initiation either. This indicates a missing element in crack initiation studies: a *length scale*. One approach is to introduce this length as an additional input parameter to the stress criterion (yielding the Theory of Critical Distances [67]) or in conjunction with the energy criterion, resulting in an incremental energy approach within Finite Fracture Mechanics [69, 70].

Another possibility is to use the CC, i.e., to combine the stress criterion and the energy criterion, which are already valid for the two extreme cases ($\beta = 0°$ and $\beta = 180°$). We then look for the minimum loading level and the corresponding crack length for which both criteria are met. The combination of the two criteria introduces a characteristic length into the problem, which is not an input parameter but rather the result of this coupling. We then obtain the initiation crack length $\ell_i$ and the GSIF $K_i$ at initiation [60, 78]:

$$\begin{cases} \ell_i = \dfrac{E\mathscr{G}_c}{A_\beta \sigma_c^2} = \dfrac{\ell_{\text{mat}}}{A_\beta}, \\[2mm] K_i = \left(\dfrac{E\mathscr{G}_c}{A_\beta}\right)^{1-\lambda} (\sigma_c)^{2\lambda-1}. \end{cases} \tag{4}$$

We note that the GSIF is homogeneous to the product of a stress and a length to the power $(1 - \lambda)$. For a straight edge, $\lambda = 1$ and the GSIF at initiation becomes $K_i = \sigma_c$ ($K_i$ is then homogeneous to a stress), thus reducing to a stress criterion. In the case of a crack, $\lambda = 1/2$ and we return to Irwin's criterion $K_i = K_{\text{Ic}} = \sqrt{E\mathscr{G}_c/A_\beta}$ ($K_i$ is then homogeneous to a critical stress intensity factor). LEFM is therefore included within the CC formulation, allowing for the study of both crack initiation and the propagation of an existing crack. The proposed formulation remains general, as it can address crack initiation with or without a singularity.

In addition to the initiation length, the combination of the two criteria introduces another characteristic length, Irwin's length $\ell_{\text{mat}} = E\mathscr{G}_c/\sigma_c^2$ [17], which is intrinsic to the material since it depends only on its elastic and fracture properties. The asymptotic approach reveals that the initiation length is actually related to Irwin's length through the dimensionless coefficient $A_\beta$, which depends on (i) the geometry (here the V-notch angle) and (ii) the loading (here the GSIF) [24, 77]. In the following, we examine how these two lengths in the CC formulation (i.e., the initiation length and Irwin's length) correspond to other characteristic lengths encountered in various fracture mechanics approaches.

## 3. Correlation with lengths involved in other fracture approaches

In this section, we focus on different approaches able to describe the nonlinear fracture resistance scaling, similarly to the CC. Even if based on different fracture description and involving different input parameters, we thus provide an insight on how the characteristic and intrinsic length scales involved in these approaches are related to the one obtained in the CC: the initiation length and Irwin's length.

Figure 2 illustrates schematically how various major techniques facilitate the emergence of a characteristic length scale, which subsequently aids in describing the nonlinear scaling observed in experiments.

For the Coupled Criterion (CC), a characteristic length emerges as the distance where both energy and stress criteria are simultaneously satisfied. This length can consistently be correlated
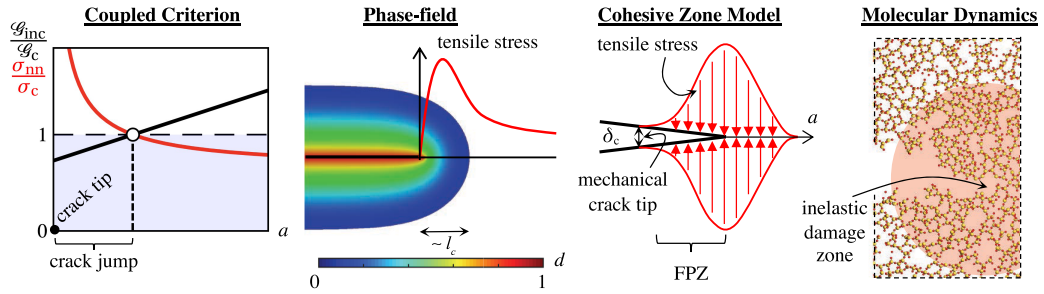
**Figure 2.** Summary of the key methods discussed, highlighting how each technique integrates material length scales into its framework and how these are reflected in simulation outcomes. In the figure $d$ represents damage, $l_c$ is the phase-field length scale, $a$ is the crack length and $\delta_c$ is the critical separation when the crack is fully open.

to Irwin's fundamental metric. Notably, studies have shown that if the initial crack is sufficiently sharp and large compared to the material's intrinsic scale, the resulting length remains constant [74]. This observation provides a possible explanation for the effectiveness of the Theory of Critical Distances (TCD): evaluating the stress at a fixed distance produces results comparable to more advanced criteria.

In smeared damage approaches, such as the Phase-Field (PF) and Thick Level Set (TLS) methods, a regularization length is inherently introduced. This regularization modifies the stress profile, resulting in a slight alteration not only near the crack tip but also in the tail of the theoretically elastic stress response for the same macroscopic equilibrium. This phenomenon raises an important question: at what distance does the calculation of experimental toughness, based on a fit to the singular solution, remain valid?

The Cohesive Zone Model (CZM) operates in a manner similar to smeared damage methods, defining the tension–separation law as an input parameter. However, CZM offers greater flexibility by allowing the critical separation to be specified, which results in a certain damage diffusion length representing the process zone ahead of the crack tip. The latter also depends on the geometry, boundary conditions and local stress state. Despite this advantage, the technique suffers from a significant limitation: it requires prior knowledge of the crack path.

Finally, particle-based methods, such as molecular dynamics (MD) and peridynamics, treat the material as a discrete system of particles. In peridynamics, the horizon explicitly defines the characteristic length scale. In atomic-scale simulations, the interaction between interatomic potentials and the realistic atomic structure leads to the emergence of a localized, inelastic zone around the crack tip [53].

This section discusses these various methods and evaluates their potential for comparison with the Coupled Criterion. We will highlight results from the literature that address the nonlinear scaling transition and examine the underlying mechanisms involved.

## 3.1. *Theory of critical distances*

The approaches based on the Theory of Critical Distances (TCD) are commonly used for engineering failure prediction [67, 79]. Since a local maximum stress criterion is unsuitable for predicting the experimentally observed size effect, even for non-singular stress fields [80], TCD compares the stress at a specified distance from a stress concentration or singular point to the material tensile strength.
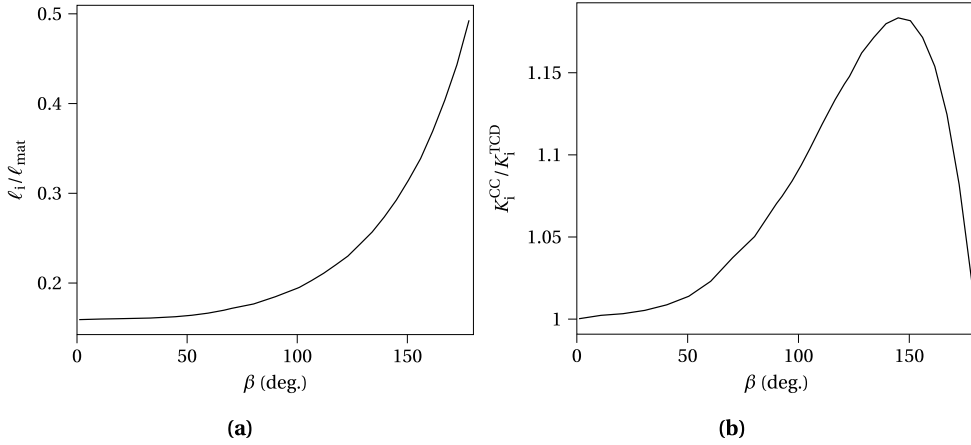
**Figure 3.** (a) Initiation length normalized by Irwin's length as a function of the V-notch angle predicted using the CC for a V-notch in an infinite medium. (b) Ratio between the GSIF obtained using either the CC ($K_i^{CC}$) or the TCD ($K_i^{TCD}$) as a function of the V-notch angle.

The CC and the TCD have been compared in various configurations, e.g., to study the fatigue limit of V-notch specimens [81]. Regardless of the notch radius, the critical distance remains constant in the TCD, whereas it decreases with increasing notch radius in the CC. By basing the TCD critical distance on Irwin's length, a relationship between the critical crack advance for both approaches—independent of material parameters—was derived. This result aligns with the fact that the initiation crack length in the CC is proportional to Irwin's length [24, 77].

Chao Correas et al. [80] demonstrated that both the CC and TCD describe the gradual transition between two stress-driven solutions for crack initiation at a spherical void (for small and large void radii, respectively). The transition between these regimes falls within the same range of void radii relative to the material characteristic length.

Campagnolo et al. [82] compared the CC to the Strain Energy Density (SED) approach for crack initiation at a V-notch under in-plane shear loading. The SED model considers the strain energy density over a control volume around the crack initiation site as the critical parameter. Both methods showed that the apparent SIF at crack initiation is proportional to powers of $K_{Ic}$ and $\sigma_c$, differing only in the proportionality factor, which depends on the notch angle in the CC and Poisson's ratio in the SED approach. Both methods predicted similar apparent SIFs at crack initiation for this configuration, with the control volume radius based on Irwin's length [82, 83].

The primary distinction between the TCD and CC is that in TCD, the characteristic length is an input parameter, while in CC it is an output derived from combining the stress and energy conditions. Several ways of nonlocal stress evaluation exist, such as integration over a volume or the use of pure nonlocal functions [84, 85]. One of the first method proposed was to evaluate the stress at a given distance from a singular point. For example, applying the TCD as a point stress criterion at a distance equal to Irwin's length ($\sigma_{nn}(\ell_{mat}) = \sigma_c$) yields:

$$K_i = (E\mathcal{G}_c)^{1-\lambda}\sigma_c^{2\lambda-1}. \tag{5}$$

This expression only differs from the one obtained using the CC by the coefficient $A_\beta$ (see Equation (4)), reflecting that the TCD disregards geometry, whereas the CC accounts for it through $A_\beta$. Figure 3 illustrates the differences between the TCD and CC in predicting crack initiation at a sharp V-notch.

The normalized initiation length obtained using the CC for different V-notch angles is shown in Figure 3a. It indicates that the initiation length using the CC is generally smaller than Irwin's length and depends on the geometry. In addition, Figure 3b shows the ratio between the GSIF obtained using the CC or the TCD as a function of the V-notch angle. Based on Equations (4) and (5), this ratio is given by $K_I^{CC}/K_I^{TCD} = A_\beta^{\lambda-1}$. Using LEFM normalization of displacement fields, a ratio of 1 is achieved for $\beta = 0°$ and $\beta = 180°$, with a non-monotonic trend as $\beta$ increases. Specifically, $A_\beta = 1$ for $\beta = 0$, decreasing with increasing $\beta$, while $\lambda$ increases from $1/2$ ($\beta = 0°$) to 1 ($\beta = 180°$). Overall, differences of less than 20% can be expected between the CC and TCD in predicting crack initiation at a V-notch in an infinite medium.

Since the TCD disregards the overall specimen geometry, questions arise about its application for small-scale specimens, where size may be smaller than Irwin's length. This method may also be unsuitable for initiation configurations driven by the energy criterion, such as transverse cracking in thin composite laminates [60, 86, 87].

## 3.2. *Phase-field*

Fracture Phase-Field (PF) models [88, 89] approximate crack discontinuities through a smeared damage field controlled by a length scale parameter ($l_c$), which defines the extent of damage. These models balance elastic energy with diffused fracture energy to identify the energetically favorable crack front, using fracture toughness ($\mathcal{G}_c$) and the regularization length ($l_c$) as primary inputs.

Both the CC and PF approaches use the critical energy release rate ($\mathcal{G}_c$) as an input parameter, but they differ in how they handle tensile strength: CC explicitly incorporates it, while PF replaces it with the regularization length ($l_c$). In simulations of notched thin ply laminate fractures, Reinoso et al. [90] showed that the CC method effectively captures the size effect and accurately predicts failure stress, whereas the PF approach slightly underestimates failure stress, with $l_c$ chosen to match the experimentally measured displacement around stress concentrators.

Early studies comparing CC and PF results [91] found good correspondence between the two methods, although the choice of $l_c$ was often based on matching maximum tensile stress under uniaxial loading to the material's tensile strength. Strobl et al. [92, 93] simulated Hertzian indentation-induced fractures using both CC and PF, noting consistent trends in crack location and critical displacement, with $l_c$ determined using the homogeneous Phase-Field solution under uniaxial tension.

Kumar et al. [94] addressed PF's tendency to overestimate critical loads at the onset of damage by explicitly incorporating a stress criterion, effectively creating a CC-inspired PF approach. Similarly, Abaza et al. [95] calibrated $l_c$ in PF models for notched ceramic specimens to match apparent stress intensity factors at crack nucleation with those obtained using CC. Jimenez et al. [96] demonstrated that for small-scale specimens, critical displacements or forces largely depend on $\mathcal{G}_c$, using CC to guide the load range selection in PF models and suggesting PF as a preliminary step for CC when the crack path is not known a priori.

A comprehensive comparison of CC and PF approaches was provided in Ref. [74], which studied tensile opening and in-plane shear fractures, proposing a correlation between tensile strength and $l_c$ that depends on the stress state:

$$\sigma_c \simeq \sigma_{max} = \eta\left(\nu, \frac{\sigma_2}{\sigma_1}, \frac{\sigma_3}{\sigma_1}\right)\sqrt{\frac{E\mathcal{G}_c}{l_c}}, \tag{6}$$

where $\eta$ accounts for the stress state. This work was later extended to antiplane shear [97]. In these studies, different aspects were compared, such as critical initiation load in tension, branching angle in simple shear, and facet spacing in antiplane shear.
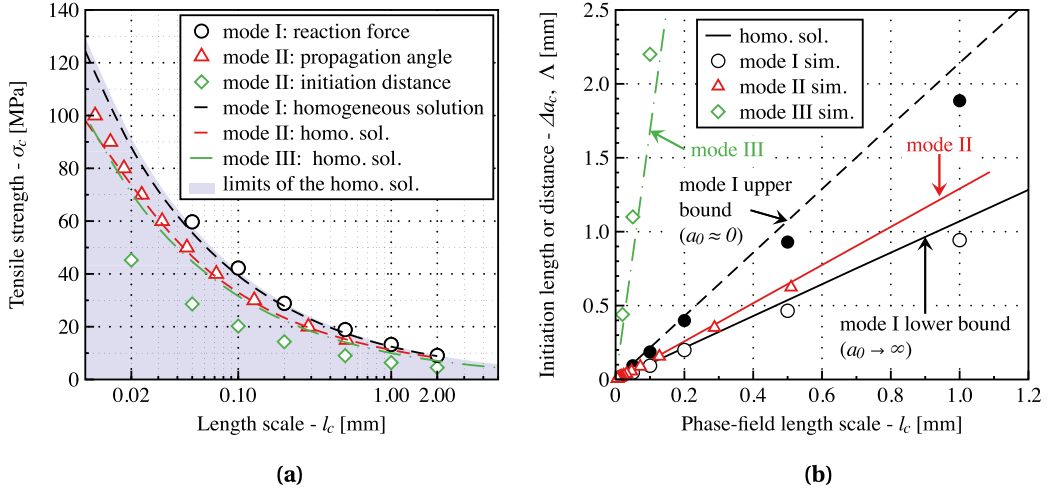
**Figure 4.** (a) Summarized correlations between the tensile strength ($\sigma_c$) and the internal length scale ($l_c$). The blue shade represents the accessible space based on the homogeneous solution. (b) Correlation between $l_c$ and the initiation lengths and characteristic distances.

The results are summarized in Figure 4. The correlations for tensile opening, in-plane, and antiplane shear fracture modes show a general trend: as the regularization length ($l_c$) decreases, the material strength ($\sigma_c$) increases. However, this relationship cannot be captured by a single master curve; instead, it forms a failure surface varying within the range defined by Equation (6), shown by the shaded area in Figure 4a. Although the initiation length $\Delta a_c$ does not explicitly appear in the PF, it is crucial for determining where the stress and energy criteria are satisfied simultaneously, with its correlation to $l_c$ being linear across different fracture modes.

The results suggest that $l_c$ serves as an intermediate parameter between Irwin's intrinsic length and the actual process zone size, though it cannot fully account for the effects of macroscopic geometry. This raises the question of whether materials have a single tensile strength (as per Rankine's theory [73]) or if the maximum tensile strength is influenced by the stress state (corresponding to another strength surface in the principal stress space).

Furthermore, studies [74, 98] showed that, similar to the CC, the PF method satisfies both energy and stress criteria due to an indirect correlation between the maximum tensile stress and $l_c$. As $l_c$ increases, the process zone enlarges, resulting in lower maximum stress and an earlier satisfaction of Griffith's criterion. Thus, higher $l_c$ values correlate with lower maximum tensile stresses needed for fracture.

Additionally, in the PF technique, the stress field is non-singular, requiring the stress tail to be slightly higher than the singular solution used in the CC to maintain equilibrium. The study of antiplane shear highlighted the need for an enhanced CC model incorporating a regularized stress field inspired by PF regularization, which would allow the CC to better address three-dimensional antiplane cracking by introducing a third parameter to account for the crack geometry, as suggested in Ref. [99].

## 3.3. *Cohesive zone*

When used in fracture mechanics, a Cohesive Zone Model (CZM) [36, 37] is designed to describe the formation and evolution of both the crack (corresponding to the traction-free region) and

the process zone ahead of the crack tip. Given, as input parameters, the material tensile and shear strengths and critical energy release rate, the CZM defines the traction–separation behavior between two surfaces.

The cohesive response is triggered once a local critical traction is reached, leading to separation and a discontinuity in the displacement field across the surfaces, governed by a distribution of traction. The traction–separation profile mechanically replicates the underlying failure mechanisms and remains active until a critical separation $\delta_c$ is reached, at which point a crack nucleates locally. This critical separation $\delta_c$ provides an intrinsic length scale that characterizes the failure process. As the separation between the two surfaces increases, the traction–separation behavior progresses to this critical point, defining a characteristic length associated with the displacement jumps necessary for crack formation.

As an example, considering only the opening mode and a bilinear traction–separation profile in a linear elastic isotropic material, the critical displacement jump is given by:

$$\delta_c = \frac{2\mathscr{G}_c}{\sigma_c} = \frac{2\sigma_c}{E}\ell_{mat} = 2\varepsilon_c\ell_{mat}, \tag{7}$$

where $\varepsilon_c$ is the material tensile strain at failure. The critical displacement jump is thus related to the material's Irwin's length and critical strain, making it an intrinsic material property.

In addition, to this characteristic length, another length is involved in CZM which is the extent of the process zone ahead of the crack. Indeed, the CZM and the CC mainly differ concerning the description of the cracking process. While the CC relies on a binary description of fracture considering two possible states, namely undamaged or cracked material, the CZM defines an intermediate state: the process zone through the description of a traction–separation profile. This process zone induces another main difference between both approaches since the stress can locally be larger than the material tensile strength in the CC whereas in CZM, the stress is always bounded by the material strength within the process zone. The process zone length depends on the Irwin's length [100, 101], but contrary to the critical displacement jump, it is not an intrinsic material property as it also depends on the specimen geometry and boundary conditions. Cornetti et al. [102] observed that for an initial crack in infinite medium or at a V-notch, the CZM process zone length was significantly different from the initiation length obtained using the CC, even if both length variations followed almost identical trends with respect to the normalized initial crack length. This analysis was then refined [103] by introducing a weight function in the stress condition of the CC in order to match the CZM. The CZM with cohesive laws exhibiting earlier softening showed satisfactory correspondence with the CC stress conditions, modified by weight functions that were elevated near the crack tip and tapered off with distance. Actually, it was shown that the difference between the failure load predicted by the CC and the CZM differs as the critical separation (and equivalently the Irwin's length) increases [104].

Nevertheless, an equivalence may possibly be determined between the CC and a given traction–separation CZM profile. Summarizing previous works aiming at the comparison between the CC and CZM [80, 105–115], it appears that there is not a unique CZM traction–separation profile that enables retrieving the failure loading and crack length predicted using the CC. The CZM traction–separation profile corresponding to the CC actually depends on the geometry, the type of loading, the cracking mechanism and thus has to be identified for a given configuration. A further comparison between the CC and the CZM was established based on another extrinsic length, i.e., the length of the crack after the unstable propagation following initiation [114]. It was shown that the range of crack lengths after unstable propagation obtained with various traction–separation profiles respectively comprised the crack length lower bound obtained using the CC, and that crack lengths similar to those obtained using the CC were obtained using a bilinear traction–separation profile in that case.

### 3.4. *Atomic scale simulations*

At the smallest scales currently accessible through computational resources to study fracture, molecular dynamics (MD) simulations [53] offer valuable insights into crack propagation by using interatomic potentials and detailed atomic structures, thus avoiding the need for additional numerical parameters. Recent studies [116, 117] have advanced our understanding of finite-size effects, revealing a critical transition in wear mechanisms at the atomic scale. Specifically, atomistic simulations show that when asperity contact junctions surpass a critical size, fracture-induced debris formation occurs, while smaller junctions result in a gradual smoothing through plastic deformation. This non-linear behavior highlights the crucial role of length scale in determining whether fracture or plastic smoothing dominates.

Later, Brochard et al. [118] specifically examined brittle failure in two materials: a simplified 2D toy model and graphene. Using molecular dynamics (MD) simulations, the authors investigate how the stress and toughness criteria contribute to the emergence of a length scale during failure. The toy model, consisting of a regular triangular lattice with harmonic interatomic interactions, allowed for a straightforward theoretical analysis of failure processes. In contrast, graphene, with its more complex atomic structure and realistic mechanical behavior, served as a case study for a real material.

For both materials, the authors use MD simulations to observe failure under different conditions, such as varying temperature, system size, and loading rate. Through these simulations, the study highlighted the emergence of a nonlinear transition length scale at the process zone near the crack tip. This process zone grew larger as the temperature increased, and the material transitions from a stress-based failure mode to one governed by energy dissipation at the crack tip. The results showed that, in graphene, this length scale and the corresponding process zone were much larger compared to the toy model, demonstrating how atomic interactions and material properties influence the scaling of strength and toughness. The simulations provided a deeper understanding of how microscopic bond-breaking processes connect to macroscopic failure behaviors, particularly in materials with varying defect types and sizes.

Chao Correas et al. [80] validated their findings by comparing the FFM approach with both experimental data and atomistic simulations. In terms of atomistic simulations, the study by Ippolito et al. [119] on $\beta$-silicon carbide is highlighted. In this work, atomistic simulations were used to create a model free of intrinsic defects by removing atoms from a crystalline lattice to simulate spherical voids. The simulations provided critical material properties, such as fracture toughness and strength, which allowed for the calculation of the Irwin's length (characteristic length scale).

Chao Correas et al. [80] found that the results of the atomistic simulations agreed with the predictions made by FFM, particularly when using the averaged stress variant. This variant provided the most accurate results when compared to the atomistic data, which eliminated scattering from experimental flaws and imperfections. This supported the use of FFM as a robust predictive tool in materials without inherent defects. The study concluded that atomistic simulations are crucial for refining predictions of failure in brittle materials, offering a close match with coupled criteria approaches like FFM in defect-free scenarios.

### 3.5. *Thick level set*

The underlying idea of the The Thick Level Set (TLS) model is to constrain the norm of the damage gradient to control the evolution of a damage field, introducing a characteristic length which represents the smallest possible distance between a fully damage point and a point where there is no damage. The characteristic length thus represents the extent of the regularization zone

around a sharp crack. Zghal et al. [120] compared the (TLS) approach to the matched asymptotic approach of the CC considering sharp or blunted notches and cavities. TLS and CC resulted in close apparent strengths for all cases provided the assumptions of the matched asymptotic approach were satisfied. However, no comparison between the TLS characteristic length and the CC initiation length was provided.

### 3.6. *Peridynamics*

Zhang et al. [121] implemented the CC to study crack initiation at circular holes within a peridynamic framework. They showed that similar strain and stress values were obtained using either peridynamics or FE modeling, except locally near the hole edge due to a skin effect arising from the incomplete non-local horizon for nodes around the hole edge. They also demonstrated that peridynamics yielded failure stresses similar to those obtained using Finite Fracture Mechanics [121]. Ultimately, in peridynamics, the characteristic length is defined by the horizon size.

   In a subsequent study, Zhang et al. [122] analyzed the stress and IERR for various horizon sizes. The main conclusion was that the skin effect influences both stress and IERR, especially for small crack lengths near a free edge. The stress and IERR values in this region are unreliable, as the local material response near a free edge differs from that in the bulk due to the incomplete horizon. They also observed that the region where stress and IERR deviate from the finite element solution increases with a larger horizon size. Ultimately, the horizon size must be set sufficiently smaller than the initiation length in the CC. Under this condition, similar stress and IERR values are obtained, indicating that peridynamics can predict similar initiation loads as the CC.

### 3.7. *Gradient elasticity*

The Gradient Elasticity (GE) model and the CC were compared to predict borehole crack initiation under combined pressure and biaxial loading [123]. It was highlighted that the CC is local in its constitutive law but non-local in the failure criterion, as both stress and energy conditions must be met simultaneously at a specific distance from the singular point or stress concentration. Conversely, the GE model is non-local in its constitutive law but local in its failure criterion, treating the governing failure parameter as the local stress concentration factor. The GE model introduces a characteristic length that defines the distance over which non-local effects act, smoothing high variations in the elastic stress field. Similar to TCD, the GE model is inapplicable below a threshold size where the internal length becomes comparable to the specimen's characteristic size. Sapora et al. [123] demonstrated that nearly identical failure stress predictions can be achieved if the internal length in the GE model is calibrated based on Irwin's length.

### 3.8. *Continuum damage model*

Continuum Damage Mechanics (CDM) [124] provides a framework for understanding how micro-damage, like micro-cracks or voids, impacts material properties at a larger scale. Kachanov [125] introduced the damage variable concept to quantify degradation from micro-defects. CDM uses constitutive models that describe stress–strain relationships and damage evolution equations based on thermodynamics to predict the transition from micro-defects to failure. Although classical CDM models uniform damage well, it faces challenges with discontinuities, prompting the development of gradient damage models [126–130], which include regularization terms to simulate phenomena like brittle fracture [131] and localized damage [132]. Methods for measuring the characteristic length of nonlocal continua have also been proposed [133].

Carrère et al. [134] compared the CC with CDM to investigate failure in adhesively bonded joints. Despite differing definitions of final failure, both models produced similar failure loads under the assumption of small displacements, as crack initiation occurs just before the specimen reaches final failure. A characteristic length emerged in the CDM, corresponding to the extent of the process zone, i.e., the region where the damage variable ranges from 0 (pristine material) to 1 (fully damaged material). At crack initiation, the process zone extent was found to be larger than the initiation length predicted by the CC, yet it followed a similar trend with respect to the material's critical energy release rate.

## 4. Discussion

The Irwin's length appears in all models that couple a stress and an energy criterion, either directly or indirectly, such as the CC, CZM, and PF models, or as a direct input parameter in models like TCD. This parameter is intrinsic to the material, obtained from a combination of other intrinsic material properties. While linking Irwin's length to the material microstructure is not always straightforward, connections can sometimes be established. For example, in polycrystalline ceramics, the intrinsic tensile strength—determined for specimens with extrinsic defects that are sufficiently small compared to the Irwin's length [23]—is related to grain size [135, 136] as well as the critical energy release rate [22]. This implies that the Irwin's length depends on grain size and other intrinsic defects present within the microstructure.

Beyond its role as an intrinsic material property, Irwin's length is crucial for the numerical implementation of the aforementioned models. It influences computational setups, such as the choice of mesh size in CZM [100, 101] and CC [77], or the selection of the regularization length in PF [74, 137].

If no length scale appears in a fracture model, it is unable to assess configurations related to crack initiation or propagation outside the assumptions of Griffith's model. A first example is Linear Elastic Fracture Mechanics, which predicts infinitely large remote stresses for a crack with vanishing size. This aligns with the assumption of a semi-infinite crack in an infinite medium, which does not hold for finite or diminishing crack lengths. A second example involves applying the TCD to specimens smaller than Irwin's length. Since TCD is based on stress evaluation at a specific distance or over a volume defined by Irwin's length, applying it to small-scale specimens is problematic, as the characteristic length becomes meaningless. A third example concerns TCD's application to energy-driven configurations without stress gradients, such as transverse cracking in laminates with thin plies. In this case, a homogeneous stress field exists within the plies transverse to the loading direction, so the TCD would predict a failure load based solely on the stress within the ply, regardless of ply thickness or the evaluation length or volume. As a result, TCD would miss the observed failure load increase with decreasing ply thickness, which is primarily controlled by energy.

Even for models coupling stress and energy conditions, there exist pathological configurations where the failure description remains incomplete. Certain cases highlight where the CC could be enhanced, specifically when the length effect is effectively "disabled" because the energy criterion predominates, causing the CC to revert to a purely energy-based criterion. Two primary configurations exhibit this behavior.

Firstly, in the presence of strong singularities [138–140], the IERR scales as $K\ell^{2\lambda-1}$ with $\lambda < 1/2$. Here, the IERR approaches infinity as the crack length tends toward zero, which means the stress criterion is always satisfied, causing the CC to revert to an energy-only criterion.

The second configuration involves a semi-infinite crack under remote anti-plane shear loading. An asymptotic approach shows that the stress criterion no longer influences the initiation

generalized stress intensity factor (GSIF), which is predicted solely based on the energy criterion, $K = (\mathcal{G}_c/A)^{1-\lambda}\sigma_c^{2\lambda-1}$, with $\lambda = 1/2$. The IERR reaches its maximum for rectilinear propagation [141–143], whereas experimental observations indicate that facets initiate at an angle inclined with respect to the primary propagation direction of the initial crack front.

In configurations where the CC fails to predict crack initiation due to the absence of a length effect, one potentially missing component could be the description of the process zone prior to initiation. Indeed, the Phase-Field approach can account for the occurrence of facets under antiplane shear [97], as observed experimentally, with the primary distinction from the CC being the presence of a process zone that develops before crack initiation. Previous studies have shown that describing this process zone is essential in PF models to accurately predict other configurations, such as along the two lips of an initial crack [74, 137, 144].

Incorporating this feature into the CC could improve its predictive capability. For example, Dominique Leguillon [145] proposed a model to describe a damage zone ahead of a V-notch prior to initiation. Alternatively, a combination of the crack regularization provided by the PF model with the CC could be implemented, as demonstrated in Ref. [99].

## 5. Conclusion

In this review, we examined characteristic lengths in fracture mechanics, with a particular focus on the Coupled Criterion framework and its interactions with other advanced fracture models. Our analysis highlighted that the CC, through coupling stress and energy criteria, uniquely clarifies the conditions under which cracks initiate across various configurations, even when dealing with theoretical scenarios that may not manifest in reality. By exploring these boundaries, we gained insights into transition behaviors that occur between configurations and the convergence of stress and energy requirements for crack initiation.

We observed that while the CC provides a comprehensive understanding of crack initiation, it lacks certain advantages of other models, such as autonomous crack path determination or the straightforward handling of multiple cracks initiating and propagating simultaneously. However, it offers valuable insights into other fracture models through the established inter-model dialogue. Our position is that fracture models can mutually benefit by extending this dialogue beyond simple comparisons of predicted failure loads obtained through different approaches.

A promising direction for the CC is to incorporate the regularization provided by the PF model or the process zone (PZ) description available in CZM. Such integration would allow for a detailed process zone description before initiation, addressing limitations in configurations where the length effect vanishes.

The development of such a dialogue between the CC and other fracture models remains an open avenue, as exemplified by the Discrete Elements Method [146, 147], which could offer a way to describe crack initiation in a manner comparable to continuum mechanics and the CC.

## Declaration of interests

The authors do not work for, advise, own shares in, or receive funds from any organization that could benefit from this article, and have declared no affiliations other than their research organizations.

## Dedication

The manuscript was written through contributions of all authors. All authors have given approval to the final version of the manuscript.

## Acknowledgments

## References

[1] A. A. Griffith, "The phenomena of rupture and flow in solids", *Philos. Trans. R. Soc. Lond. A* **221** (1921), no. 582-593, p. 163-198.

[2] A. A. Griffith, "The theory of rupture", in *First International Congress on Applied Mechanics*, Waltman, 1924, p. 55-63.

[3] L. da Vinci, *Codex Atlanticus*, Bibilioteca Ambrosiana, 1504, https://en.wikipedia.org/wiki/Codex_Atlanticus.

[4] E. Williams, "Some observations of Leonardo, Galileo, Mariotte and others relative to size effect", *Ann. Sci.* **13** (1957), no. 1, p. 23-29.

[5] G. Galilei, *Discourses and Mathematical Demonstrations Relating to Two New Sciences*, Louis Elsevier, Leida (Leiden), 1638.

[6] D. Kirkaldy, *Results of an Experimental Inquiry into the Tensile Strength and Other Properties of Various Kinds of Wrought-iron and Steel*, Private Publication, London, 1864.

[7] E. Mariotte, *Traité du mouvement des eaux et des autres corps fluides*, Chez Jean Jombert, Paris, 1886.

[8] F. T. Peirce, "Theorems on the strength of long and of composite specimens", *J. Text Inst. Trans.* **17** (1926), no. 7, p. T355-T368.

[9] L. C. H. Tippett, "On the extreme individuals and the range of samples taken from a normal population", *Biometrika* **17** (1925), p. 364-387.

[10] W. Weibull, "Statistical theory of the strength of materials", *Proc. R. Acad. Eng. Sci.* **15** (1939), no. 1, p. 1-45.

[11] W. Weibull, "The phenomenon of rupture in solids", *IVA Handlingar* **153** (1939), p. 1-55.

[12] A. M. Freudenthal, "The statistical aspect of fatigue of materials", *Proc. R. Soc. Lond. Ser. A* **187** (1946), no. 1011, p. 416-429.

[13] P. Kittl, G. Díaz, "Size effect on fracture strength in the probabilistic strength of materials", *Reliab. Eng. Syst. Saf.* **28** (1990), no. 1, p. 9-21.

[14] A. G. Evans, "A general approach for the statistical analysis of multiaxial fracture", *J. Am. Ceram. Soc.* **61** (1978), no. 7-8, p. 302-308.

[15] F. M. Beremin, A. Pineau, F. Mudry, J. C. Devaux, Y. DEscatha, P. Ledermann, "A local criterion for cleavage fracture of a nuclear pressure vessel steel", *Metall. Trans. A* **14** (1983), p. 2277-2287.

[16] Y. Lei, N. P. O'Dowd, E. P. Busso, G. A. Webster, "Weibull stress solutions for 2-D cracks in elastic and elastic-plastic materials", *Int. J. Fract.* **89** (1998), p. 245-268.

[17] G. R. Irwin, *Fracture*, Springer, Berlin, Heidelberg, 1958.

[18] Z. P. Bažant, "Size effect in blunt fracture: concrete, rock, metal", *J. Eng. Mech.* **110** (1984), no. 4, p. 518-535.

[19] Z. P. Bažant, J. Kim, P. Pfeiffer, "Nonlinear fracture properties from size effect tests", *J. Struct. Eng.* **112** (1986), no. 2, p. 289-307.

[20] Z. P. Bažant, "Size effect on structural strength: a review", *Arch. Appl. Mech.* **69** (1999), p. 703-725.

[21] H. Kimoto, S. Usami, H. Miyata, "Flaw size dependence in fracture stress of glass and polycrystalline ceramics", *Trans. Jpn. Soc. Mech. Eng. Ser. A* **51** (1985), no. 471, p. 2482-2488.

[22] S. Usami, H. Kimoto, I. Takahashi, S. Shida, "Strength of ceramic materials containing small flaws", *Eng. Frac. Mech.* **23** (1986), no. 4, p. 745-761.

[23] D. Leguillon, E. Martin, "Prediction of multi-cracking in sub-micron films using the coupled criterion", *Int. J. Frac.* **209** (2018), p. 187-202.

[24] E. Martin, D. Leguillon, O. Sevecek, R. Bermejo, "Understanding the tensile strength of ceramics in the presence of small critical flaws", *Eng. Frac. Mech.* **201** (2018), p. 167-175.

[25] A. Doitrand, A. Sapora, "Nonlinear implementation of finite fracture mechanics: a case study on notched Brazilian disk samples", *Int. J. Non-Linear Mech.* **119** (2020), article no. 103245.

[26] A. Sapora, A. R. Torabi, S. Etesam, P. Cornetti, "Finite fracture mechanics crack initiation from a circular hole", *Fatigue Frac. Eng. Mater. Struct.* **41** (2018), no. 7, p. 1627-1636.

[27] J. Luo, J. Wang, E. Bitzek *et al.*, "Size-dependent brittle-to-ductile transition in silica glass nanofibers", *Nano Lett.* **16** (2016), no. 1, p. 105-113.

[28] Z. P. Bažant, M. T. Kazemi, "Size effect in fracture of ceramics and its use to determine fracture energy and effective process zone length", *J. Am. Ceram. Soc.* **73** (1990), no. 7, p. 1841-1853.

[29] Z. P. Bažant, I. M. Daniel, Z. Li, "Size effect and fracture characteristics of composite laminates", *J. Eng. Mater. Technol.* **118** (1996), no. 3, p. 317-324.

[30] S. Aicher, "Process zone length and fracture energy of spruce wood in mode-I from size effect", *Wood Fiber Sci.* **42** (2010), no. 2, p. 237-247.

[31] S. P. Shah, S. E. Swartz, "Fracture of concrete and rock", in *SEM-RILEM International Conference*, Springer, New York, 1987.

[32] S. Keten, Z. Xu, B. Ihle, M. J. Buehler, "Nanoconfinement controls stiffness, strength and mechanical toughness of $\beta$-sheet crystals in silk", *Nat. Mater.* **9** (2010), no. 4, p. 359-367.

[33] J. P. Dempsey, R. M. Adamson, S. V. Mulmule, "Scale effects on the in-situ tensile strength and fracture of ice. Part II: First-year sea ice at Resolute, NWT", *Int. J. Frac.* **95** (1999), no. 1, p. 347-366.

[34] G. R. Irwin, "Fracture dynamics", in *Fracturing of Metals*, American Society for Metals, Cleveland, 1948, p. 147-166.

[35] E. Orowan, "Fracture and strength of solids", *Rep. Prog. Phys.* **12** (1949), p. 185-232.

[36] G. I. Barenblatt, "The formation of equilibrium cracks during brittle fracture. General ideas and hypotheses. Axially-symmetric cracks", *J. Appl. Math. Mech.* **23** (1959), no. 3, p. 622-636.

[37] D. S. Dugdale, "Yielding of steel sheets containing slits", *J. Mech. Phys. Solids* **8** (1960), no. 2, p. 100-104.

[38] J. F. Labuz, S. P. Shah, C. H. Dowding, "Post peak tensile load-displacement response and the fracture process zone in rock", in *The 24th US Symposium on Rock Mechanics (USRMS)*, Association of Engineering Geologists, 1983.

[39] W. Chengyong, L. Peide, H. Rongsheng, S. Xiutang, "Study of the fracture process zone in rock by laser speckle interferometry", *Int. J. Rock Mech. Min. Sci. Geomech. Abstr.* **27** (1990), no. 1, p. 65-69.

[40] E. Denarie, V. E. Saouma, A. Iocco, D. Varelas, "Concrete fracture process zone characterization with fiber optics", *J. Eng. Mech.* **127** (2001), no. 5, p. 494-502.

[41] J. J. Du, A. S. Kobayashi, N. M. Hawkins, "An experimental-numerical analysis of fracture process zone in concrete fracture specimens", *Eng. Frac. Mech.* **35** (1990), no. 1-3, p. 15-27.

[42] Z. K. Guo, A. S. Kobayashi, N. M. Hawkins, "Further studies on fracture process zone for mode I concrete fracture", *Eng. Frac. Mech.* **46** (1993), no. 6, p. 1041-1049.

[43] C.-T. Yu, A.-S. Kobayashi, "Fracture process zone associated with mixed mode fracture of SiCw/Al2O3", *J. Non-Cryst. Solids* **177** (1994), p. 26-35.

[44] A. Zang, F. C. Wagner, S. Stanchits, C. Janssen, G. Dresen, "Fracture process zone in granite", *J. Geophys. Res.: Solid Earth* **105** (2000), no. B10, p. 23651-23661.

[45] K. Otsuka, H. Date, "Fracture process zone in concrete tension specimen", *Eng. Frac. Mech.* **65** (2000), no. 2-3, p. 111-131.

[46] W. K. Zietlow, J. F. Labuz, "Measurement of the intrinsic process zone in rock using acoustic emission", *Int. J. Rock Mech. Min. Sci.* **35** (1998), no. 3, p. 291-299.

[47] J. F. Labuz, S. P. Shah, C. H. Dowding, "The fracture process zone in granite: evidence and effect", *Int. J. Rock Mech. Min. Sci. Geomech. Abstr.* **24** (1987), p. 235-246.

[48] A. Neimitz, E. C. Aifantis, "On the size and shape of the process zone", *Eng. Frac. Mech.* **26** (1987), no. 4, p. 491-503.

[49] L. Cedolin, S. D. Poli, I. Iori, "Experimental determination of the fracture process zone in concrete", *Cem. Concr. Res.* **13** (1983), no. 4, p. 557-567.

[50] J. M. Vermilye, C. H. Scholz, "The process zone: A microstructural view of fault growth", *J. Geophys. Res.: Solid Earth* **103** (1998), no. B6, p. 12223-12237.

[51] Y. Yu, W. Zeng, W. Liu, H. Zhang, X. Wang, "Crack propagation and fracture process zone (FPZ) of wood in the longitudinal direction determined using digital image correlation (DIC) technique", *Remote Sens.* **11** (2019), no. 13, p. 1-13.

[52] K. Haidar, G. Pijaudier-Cabot, J.-F. Dubé, A. Loukili, "Correlation between the internal length, the fracture process zone and size effect in model materials", *Mater. Struct.* **38** (2005), no. 2, p. 201-210.

[53] C. L. Rountree, D. Bonamy, D. Dalmas, S. Prades, R. K. Kalia, C. Guillot, E. Bouchaud, "Fracture in glass via molecular dynamics simulations and atomic force microscopy experiments", *Phys. Chem. Glas.: Eur. J. Glass Sci. Technol. B* **51** (2010), no. 2, p. 127-132.

[54] Z. Brooks, *Fracture process zone: Microstructure and nanomechanics in quasi-brittle materials*, Phd thesis, Massachusetts Institute of Technology, 2013.

[55] J. Réthoré, R. Estevez, "Identification of a cohesive zone model from digital images at the micron-scale", *J. Mech. Phys. Solids* **61** (2013), no. 6, p. 1407-1420.

[56] P.-P. Cortet, S. Santucci, L. Vanel, S. Ciliberto, "Slow crack growth in polycarbonate films", *Europhys. Lett.* **71** (2005), no. 2, p. 242-248.

[57] W. Döll, "Optical interference measurements and fracture mechanics analysis of crack tip craze zones", *Adv. Polym. Sci.* **52-53** (1983), p. 105-168.

[58] W. Döll, L. Könczöl, "Micromechanics of fracture under static and fatigue loading: Optical interferometry of crack tip craze zones", *Adv. Poly. Sci.* **91-92** (1990), p. 137-214.

[59]  T. A. Schaedler, A. J. Jacobsen, A. Torrents, A. E. Sorensen, J. Lian, J. R. Greer, L. Valdevit, W. B. Carter, "Ultralight metallic microlattices", *Science* **334** (2011), no. 6058, p. 962-965.

[60]  D. Leguillon, "Strength or toughness? A criterion for crack onset at a notch", *Eur. J. Mech.—A/Solids* **21** (2002), no. 1, p. 61-72.

[61]  A. Parvizi, K. W. Garrett, J. E. Bailey, "Constrained cracking in glass fibre-reinforced epoxy cross-ply laminates", *J. Mater. Sci.* **13** (1978), p. 195-201.

[62]  G. Lamé, B. Clapeyron, "Mémoire sur l'équilibre intérieur des corps solides homogènes", *J. Reine Angew. Math.* **7** (1831), p. 381-413.

[63]  H. Neuber, "Theorie der technischen Formzahl", *Forsch. Ingenieurwes. A* **7** (1936), no. 6, p. 271-274.

[64]  R. E. Peterson, *Methods of Correlating Data from Fatigue Tests of Stress Concentration Specimens*, Macmillan, New York, 1938, Stephen Timoshenko Anniversary Volume, 179 pages.

[65]  J. M. Whitney, R. J. Nuismer, "Stress fracture criteria for laminated composites containing stress concentrations", *J. Compos. Mater.* **8** (1974), no. 3, p. 253-265.

[66]  K. Tanaka, "Engineering formulae for fatigue strength reduction due to crack-like notches", *Int. J. Frac.* **22** (1983), no. 2, p. R39-R46.

[67]  D. Taylor, *The Theory of Critical Distances*, Elsevier Science Ltd, Oxford, 2007.

[68]  J. Aveston, A. Kelly, "Theory of multiple fracture of fibrous composites", *J. Mater. Sci.* **8** (1973), no. 3, p. 352-362.

[69]  Z. Hashin, "Finite thermoelastic fracture criterion with application to laminate cracking analysis", *J. Mech. Phys. Solids* **44** (1996), no. 7, p. 1129-1145.

[70]  J. A. Nairn, "Fracture mechanics of composites with residual stresses, traction-loaded cracks, and imperfect interfaces", in *Fracture of Polymers, Composites and Adhesives* (J. G. Williams, A. Pavan, eds.), European Structural Integrity Society, vol. 27, Elsevier, Les Diablerets, 2000, p. 111-121.

[71]  P. Weißgraeber, D. Leguillon, W. Becker, "A review of finite fracture mechanics: crack initiation at singular and non-singular stress raisers", *Arch. Appl. Mech.* **86** (2016), no. 1-2, p. 375-401.

[72]  A. Doitrand, T. Duminy, H. Girard, X. Chen, "A review of the coupled criterion", *J. Theor. Comput. Appl. Mech.* (2024), article no. 11072.

[73]  W. J. M. Rankine, "II. On the stability of loose earth", *Philos. Trans. R. Soc. Lond.* **147** (1857), p. 9-27.

[74]  G. Molnár, A. Doitrand, R. Estevez, A. Gravouil, "Toughness or strength? Regularization in phase-field fracture explained by the coupled criterion", *Theor. Appl. Frac. Mech.* **109** (2020), article no. 102736.

[75]  A. Doitrand, R. Henry, J. Chevalier, S. Meille, "Revisiting the strength of micron-scale ceramic platelets", *J. Am. Ceramic Soc.* **103** (2020), p. 6991-7000.

[76]  D. Leguillon, E. Sanchez-Palencia, *Computation of Singular Solutions in Elliptic Problems and Elasticity*, Wiley, USA, 1987.

[77]  A. Doitrand, E. Martin, D. Leguillon, "Numerical implementation of the coupled criterion: Matched asymptotic and full finite element approaches", *Finite Element Anal. Des.* **168** (2020), article no. 103344.

[78]  D. Leguillon, D. Quesada, C. Putot, E. Martin, "Prediction of crack initiation at blunt notches and cavities—size effects", *Eng. Frac. Mech.* **74** (2007), no. 15, p. 2420-2436.

[79]  D. Taylor, P. Cornetti, N. Pugno, "The fracture mechanics of finite crack extension", *Eng. Frac. Mech.* **72** (2005), no. 7, p. 1021-1038.

[80]  A. Chao Correas, M. Corrado, A. Sapora, P. Cornetti, "Size-effect on the apparent tensile strength of brittle materials with spherical cavities", *Theor. Appl. Frac. Mech.* **116** (2021), article no. 103120.

[81]  Y. Liu, C. Deng, B. Gong, "Discussion on equivalence of the theory of critical distances and the coupled stress and energy criterion for fatigue limit prediction of notched specimens", *Int. J. Fatigue* **131** (2020), article no. 105236.

[82]  A. Campagnolo, F. Berto, D. Leguillon, "Fracture assessment of sharp V-notched components under Mode II loading: a comparison among some recent criteria", *Theor. Appl. Frac. Mech.* **85** (2016), p. 217-226.

[83]  Z. Yosibash, A. Bussiba, I. Gilad, "Failure criteria for brittle elastic materials", *Int. J. Frac.* **125** (2004), p. 307-333.

[84]  B. Gillham, A. Yankin, F. McNamara *et al.*, "Tailoring the theory of critical distances to better assess the combined effect of complex geometries and process-inherent defects during the fatigue assessment of SLM Ti-6Al-4V", *Int. J. Fatigue* **172** (2023), article no. 107602.

[85]  A. K. Matpadi Raghavendra, V. Maurel, L. Marcin, H. Proudhon, "Fatigue life prediction at mesoscopic scale of samples containing casting defects: A novel energy based non-local model", *Int. J. Fatigue* **188** (2024), article no. 108485.

[86]  A. Doitrand, G. Molnár, D. Leguillon, E. Martin, N. Carrère, "Dynamic crack initiation assessment with the coupled criterion", *Eur. J. Mech.—A/Solids* **93** (2022), article no. 104483.

[87]  Z. Hamam, N. Godin, P. Reynaud, C. Fusco, N. Carrére, A. Doitrand, "Transverse cracking induced acoustic emission in carbon fiber-epoxy matrix composite laminates", *Materials* **15** (2022), p. 1-15.

[88]  B. Bourdin, G. A. Francfort, J. J. Marigo, "Numerical experiments in revisited brittle fracture", *J. Mech. Phys. Solids* **48** (2000), no. 4, p. 797-826.

[89]  B. Bourdin, G. A. Francfort, J.-J. Marigo, *The Variational Approach to Fracture*, Springer, Netherlands, 2008.

[90] J. Reinoso, A. Arteiro, M. Paggi, P. P. Camanho, "Strength prediction of notched thin ply laminates using finite fracture mechanics and the phase field approach", *Compos. Sci. Technol.* **150** (2017), p. 205-216.

[91] J. Bleyer, R. Alessi, "Phase-field modeling of anisotropic brittle fracture including several damage mechanisms", *Comput. Methods Appl. Mech. Eng.* **336** (2018), p. 213-236.

[92] M. Strobl, P. Dowgiallo, T. Seelig, "Analysis of Hertzian indentation fracture in the framework of finite fracture mechanics", *Int. J. Frac.* **206** (2017), p. 67-79.

[93] M. Strobl, T. Seelig, "Phase field modeling of Hertzian indentation fracture", *J. Mech. Phys. Solids* **143** (2020), article no. 104026.

[94] A. Kumar, B. Bourdin, G. A. Francfort, O. Lopez-Pamies, "Revisiting nucleation in the phase-field approach to brittle fracture", *J. Mech. Phys. Solids* **142** (2020), article no. 104027.

[95] A. Abaza, J. Laurencin, A. Nakajo, S. Meille, J. Debayle, D. Leguillon, "Prediction of crack nucleation and propagation in porous ceramics using the phase-field approach", *Theor. Appl. Frac. Mech.* **119** (2022), article no. 103349.

[96] S. Jiménez-Alfaro, J. Reinoso, D. Leguillon, C. Maurini, "Finite fracture mechanics from the macro- to the micro-scale. comparison with the phase field model", *Procedia Struct. Integr.* **42** (2022), p. 553-560, 23 European Conference on Fracture.

[97] G. Molnár, A. Doitrand, V. Lazarus, "Phase-field simulation and coupled criterion link echelon cracks to internal length in antiplane shear", *J. Mech. Phys. Solids* **188** (2024), article no. 105675.

[98] P. K. Kristensen, C. F. Niordson, E. Martinez-Paneda, "An assessment of phase field fracture: crack initiation and growth", *Philos. Trans. R. Soc. A* **379** (2021), no. 2203, article no. 20210021.

[99] A. Doitrand, G. Molnár, "Understanding regularized crack initiation through the lens of finite fracture mechanics", preprint, 2024, https://doi.org/10.21203/rs.3.rs-4583166/v1.

[100] G. Alfano, M. A. Crisfield, "Finite element interface models for the delamination analysis of laminated composites: mechanical and computational issues", *Int. J. Numer. Methods Eng.* **50** (2001), no. 7, p. 1701-1736.

[101] G. Alfano, "On the influence of the shape of the interface law on the application of cohesive-zone models", *Compos. Sci. Technol.* **66** (2006), no. 6, p. 723-730.

[102] P. Cornetti, A. Sapora, A. Carpinteri, "Short cracks and V-notches: finite fracture mechanics vs cohesive crack model", *Eng. Frac. Mech.* **168** (2016), p. 2-12.

[103] P. Cornetti, M. Munoz-Reja, A. Sapora, A. Carpinteri, "Finite fracture mechanics and cohesive crack model: weight functions vs cohesive laws", *Int. J. Solids Struct.* **156-157** (2019), p. 126-136.

[104] E. Martin, T. Vandellos, D. Leguillon, N. Carrère, "Initiation of edge debonding: coupled criterion versus cohesive zone model", *Int. J. Frac.* **199** (2016), p. 157-168.

[105] C. Henninger, D. Leguillon, E. Martin, "Crack initiation at a V-notch—comparison between a brittle fracture criterion and the Dugdale cohesive model", *C. R. Méc.* **335** (2007), no. 7, p. 388-393.

[106] S. Murer, D. Leguillon, "Static and fatigue failure of quasi-brittle materials at a V-notch using a Dugdale model", *Eur. J. Mech.—A/Solids* **29** (2010), no. 2, p. 109-118.

[107] I. G. García, M. Paggi, V. Mantivc, "Fiber-size effects on the onset of fiber–matrix debonding under transverse tension: A comparison between cohesive zone and finite fracture mechanics models", *Eng. Frac. Mech.* **115** (2014), p. 96-110.

[108] P. Cornetti, M. Corrado, L. De Lorenzis, A. Carpinteri, "An analytical cohesive crack modeling approach to the edge debonding failure of FRP-plated beams", *Int. J. Solids Struct.* **53** (2015), p. 92-106.

[109] N. Stein, P. Weissgraeber, W. Becker, "A model for brittle failure in adhesive lap joints of arbitrary joint configuration", *Compos. Struct.* **133** (2015), p. 707-718.

[110] L. Távara, I. G. Garcia, R. Vodicka, C. G. Panagiotopoulos, V. Mantivc, "Revisiting the problem of debond initiation at fibre-matrix interface under transversal biaxial loads - a comparison of several non-classical fracture mechanics approaches", *Trans Tech Publications, Ltd* **713** (2016), p. 232-235.

[111] R. Dimitri, P. Cornetti, V. Mantic, M. Trullo, L. De Lorenzis, "Mode-I debonding of a double cantilever beam: a comparison between cohesive crack modeling and finite fracture mechanics", *Int. J. Solids Struct.* **124** (2017), p. 57-72.

[112] P. L. Rosendahl, P. Weissgraeber, N. Stein, W. Becker, "Asymmetric crack onset at open-holes under tensile and in-plane bending loading", *Int. J. Solids Struct.* **113-114** (2017), p. 10-23.

[113] T. Gentieu, J. Jumel, A. Catapano, J. Broughton, "Size effect in particle debonding: comparisons between finite fracture mechanics and cohesive zone model", *J. Compos. Mater.* **53** (2018), no. 14, p. 1941-1954.

[114] A. Doitrand, R. Estevez, D. Leguillon, "Comparison between cohesive zone and coupled criterion modeling of crack initiation in rhombus hole specimens under quasi-static compression", *Theor. Appl. Frac. Mech.* **99** (2019), p. 51-59.

[115] M. Munoz-Reja, P. Cornetti, L. Távara, V. Mantivc, "Interface crack model using finite fracture mechanics applied to the double pull-push shear test", *Int. J. Solids Struct.* **188-189** (2020), p. 56-73.

[116] R. Aghababaei, D. H. Warner, J.-F. Molinari, "Critical length scale controls adhesive wear mechanisms", *Nat. Commun.* **7** (2016), no. 1, article no. 11816.

[117] R. Aghababaei, D. H. Warner, J.-F. Molinari, "On the debris-level origins of adhesive wear", *Proc. Nat. Acad. Sci.* **114** (2017), no. 30, p. 7935-7940.

[118] L. Brochard, S. Souguir, K. Sab, "Scaling of brittle failure: strength versus toughness", *Int. J. Frac.* **210** (2018), p. 153-166.

[119] M. Ippolito, A. Mattoni, N. Pugno, L. Colombo, "Failure strength of brittle materials containing nanovoids", *Phys. Rev. B* **75** (2007), no. 22, article no. 224110.

[120] J. Zghal, K. Moreau, N. Moës, D. Leguillon, C. Stolz, "Analysis of the failure at notches and cavities in quasi-brittle media using the Thick Level Set damage model and comparison with the coupled criterion", *Int. J. Frac.* **211** (2018), p. 253-280.

[121] H. Zhang, P. Qiao, "A coupled peridynamic strength and fracture criterion for openhole failure analysis of plates under tensile load", *Eng. Frac. Mech.* **204** (2018), p. 103-118.

[122] H. Zhang, P. Qiao, L. Lu, "Failure analysis of plates with singular and non-singular stress raisers by a coupled peridynamic model", *Int. J. Mech. Sci.* **157-158** (2019), p. 446-456.

[123] A. Sapora, G. Efremidis, P. Cornetti, "Comparison between two nonlocal criteria: a case study on pressurized holes", *Procedia Struct. Integr.* **33** (2021), p. 456-464.

[124] J. Lemaitre, "How to use damage mechanics", *Nucl. Eng. Design* **80** (1984), no. 2, p. 233-245.

[125] L. M. Kachanov, "Rupture time under creep conditions", *Izvestia Akademii Nauk SSSR, Otdelenie tekhnicheskich nauk* (1958), no. 8, p. 26-31, Leningrad University (translated) (in Russian) reprint: https://doi.org/10.1023/A:1018671022008.

[126] G. Pijaudier-Cabot, Z. P. Bažant, "Nonlocal damage theory", *J. Eng. Mech.* **113** (1987), no. 10, p. 1512-1533.

[127] A. Benallal, R. Billardon, J. Lemaitre, "Continuum damage mechanics and local approach to fracture: numerical procedures", *Comput. Methods Appl. Mech. Eng.* **92** (1991), no. 2, p. 141-155.

[128] R. de Borst, A. Benallal, O. M. Heeres, "A gradient-enhanced damage approach to fracture", *J. Phys. IV* **6** (1996), no. C6, p. 491-502.

[129] R. H. J. Peerlings, R. de Borst, W. A. M. Brekelmans, J. H. P. de Vree, "Gradient enhanced damage for quasi-brittle materials", *Int. J. Numer. Methods Eng.* **39** (1996), no. 19, p. 3391-3403.

[130] R. H. J. Peerlings, R. de Borst, W. A. M. Brekelmans, M. G. D. Geers, "Gradient-enhanced damage modelling of concrete fracture", *Mech. Cohesive-frict. Mater. Int. J. Exp. Model. Comput. Mater. Structures* **3** (1998), no. 4, p. 323-342.

[131] R. de Borst, "Fracture in quasi-brittle materials: a review of continuum damage-based approaches", *Eng. Frac. Mech.* **69** (2002), no. 2, p. 95-112.

[132] M. G. D. Geers, R. de Borst, W. A. M. Brekelmans, R. H. J. Peerlings, "Strain-based transient-gradient damage model for failure analyses", *Comput. Methods Appl. Mech. Eng.* **160** (1998), no. 1-2, p. 133-153.

[133] Z. P. Bažant, G. Pijaudier-Cabot, "Measurement of characteristic length of nonlocal continuum", *J. Eng. Mech.* **115** (1989), no. 4, p. 755-767.

[134] N. Carrère, E. Martin, D. Leguillon, "Comparison between models based on a coupled criterion for the prediction of the failure of adhesively bonded joints", *Eng. Frac. Mech.* **138** (2015), p. 185-201.

[135] E. O. Hall, "The deformation and ageing of mild steel: III discussion of results", *Proc. Phys. Soc. Section B* **64** (1951), no. 9, p. 747-753.

[136] N. J. Petch, "The cleavage strength of polycrystals", *J. Iron Steel Inst.* **174** (1953), p. 25-28.

[137] G. Molnár, A. Doitrand, A. Jaccon, B. Prabel, A. Gravouil, "Thermodynamically consistent linear-gradient damage model in Abaqus", *Eng. Frac. Mech.* **266** (2022), article no. 108390.

[138] D. Leguillon, C. Lacroix, E. Martin, "Interface debonding ahead of a primary crack", *J. Mech. Phys. Solids* **48** (2000), no. 10, p. 2137-2161.

[139] D. Leguillon, S. Murer, "Fatigue crack nucleation at a stress concentration point", in *CP2012 Conference Proceedings*, vol. 46, ESIS Publishing House, 2012, https://www.gruppofrattura.it/ocs/index.php/esis/CP2012/paper/viewFile/9235/5996.

[140] M. T. Aranda, D. Leguillon, "Prediction of failure of hybrid composites with ultra-thin carbon/epoxy layers using the Coupled Criterion", *Eng. Frac. Mech.* **281** (2023), article no. 109053.

[141] B. Mittelman, Z. Yosibash, "Asymptotic analysis of the potential energy difference because of a crack at a V-notch edge in a 3D domain", *Eng. Frac. Mech.* **131** (2014), p. 232-256.

[142] B. Mittelman, Z. Yosibash, "Energy release rate cannot predict crack initiation orientation in domains with a sharp V-notch under mode III loading", *Eng. Frac. Mech.* **141** (2015), p. 230-241.

[143] A. Doitrand, D. Leguillon, G. Molnár, V. Lazarus, "Revisiting facet nucleation under mixed mode I+III loading with T-stress and mode-dependent fracture properties", *Int. J. Frac.* **242** (2023), p. 85-106.

[144] M. Klinsmann, D. Rosato, M. Kamlah, R. M. McMeeking, "An assessment of the phase field formulation for crack growth", *Comput. Methods Appl. Mech. Eng.* **294** (2015), p. 313-330.

[145] D. Leguillon, Z. Yosibash, "Failure initiation at V-notch tips in quasi-brittle materials", *Int. J. Solids Struct.* **122-123** (2017), p. 1-13.

[146] D. André, J. Girardot, C. Hubert, "A novel DEM approach for modeling brittle elastic media based on distinct lattice spring model", *Comput. Methods Appl. Mech. Eng.* **350** (2019), p. 100-122.

[147] M. Voisin-Leprince, J. Garcia-Suarez, G. Anciaux, J.-F. Molinari, "Two-scale concurrent simulations for crack propagation using FEM–DEM bridging coupling", *Comput. Part. Mech.* **11** (2024), no. 5, p. 2235-2243.